

# KINEMATIC SPINDLES FOR PORTABLE ROUNDNESS INSTRUMENTS

Eric Wolsing, King-Fu Hii, R Ryan Vallance

Precision Systems Laboratory, University of Kentucky, Lexington, KY

## Abstract

This paper describes the design and analysis of a kinematic spindle for a rotating sensitive direction portable roundness instrument. The instrument will employ contact profilometry and reversal techniques with a kinematically coupled spindle for an application such as quality assurance in the production- of engine bores. Reversal requires a spindle configuration exhibiting low asynchronous errors. The spindle uses exact constraint principles (kinematic) by establishing one axial contact point and four radial contact points. Explanation of the spindle drive arrangement is provided including (1) experiments for measuring magnetic preload, and (2) a demonstration of the relationship between z-axis magnetic preloading and radial preloading on the spindle's four radial contact points.

**Keywords:** Kinematic, spindle, exact constraint, roundness, metrology

## Introduction

Roundness is a critical geometric tolerance in precision machines and products [1]. Any precision product utilizing cylindrical bores is likely concerned with form errors in the manufactured cylindrical surface. For instance, piston bores in engine blocks require tight roundness and cylindricity tolerances to generate maximum power and operate efficiently. A precise, robust, but inexpensive method for measuring the roundness of engine bores on the production line could therefore benefit engine manufacturers.

Instruments used for measuring roundness require spindles with low asynchronous errors in the axis of rotation. If synchronous errors are present in the axis of rotation or artifact, they may be separated from the measured profile using reversal techniques as described by Donaldson [2] and by Estler and Hocken [3]. Therefore, a kinematic spindle, which exhibits low asynchronous error but higher synchronous errors, can be used in conjunction with a reversal technique.

This paper presents some aspects of designing a portable prototype instrument suitable for measuring roundness profiles. The instrument employs a kinematically constrained spindle shaft as illustrated in Fig 1. The spindle is exactly constrained [4] using an arrangement of four radial constraints and one axial constraint. Curvature matching at the contact points is achieved with hemispheres contacting the surface of a bored hole. Preload in the axial direction is by permanent magnets (not shown in Fig 1) and by a flexure in the radial direction.

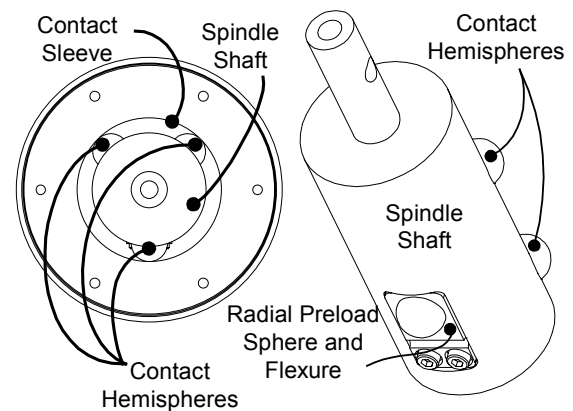


**Fig 1: Kinematic Spindle Arrangement**

Hii [5] investigated a kinematically constrained spindle shafts (without curvature matching) and demonstrated that they are capable of low asynchronous errors ( $\sim 25\text{-}50$  nm). The synchronous errors are repeatable and directly related to the roundness profile of the spindle shaft and bore. Hii et al. [6] rotated the kinematically constrained shaft using a lightly tensioned belt wrapped around the spindle's shaft and driven with a pulley. This approach introduced errors associated with compliancy at the radial contact points and fluctuations in the belt tension.

In this paper, we describe an alternative embodiment using curvature matching and analyze a method for rotating the shaft by applying nearly pure torque through the axial contact point. This is achieved by friction-based surface tractions within the contact area at the axial constraint. Since permanent magnets preload the axial contact point, the normal force producing friction depends upon the magnitude of the magnetic force minus the weight of the spindle shaft. Therefore, experiments quantifying

the magnetic preload as a function of the distance between an array of magnets and a steel plate are presented.

To prevent slipping at the axial contact point while rotating the shaft, the peak transmissible torque must exceed the torque due to friction at the radial contact points. Possible designs are analyzed by integrating data from the magnetic preload measurements with an analytical model. This determines a suitable preload force in the radial direction that does not produce exceedingly high friction and lead to slipping at the axial constraint.

### Description of the Prototype Instrument

A cross section of the prototype instrument is illustrated in Fig 2. The drive arrangement is clearly depicted in the upper portion of Fig 2 at the Z-axis contact. A knurled wheel is turned by hand, and torque is transmitted via surface tractions between the Z-axis contact hemisphere and the steel plate. The kinematically constrained shaft rotates within the spindle bore. The radial contact spheres preferably slide on a low-friction contact sleeve. A contact probe (not shown) would be affixed to the bottom of the shaft to reside within the test bore.

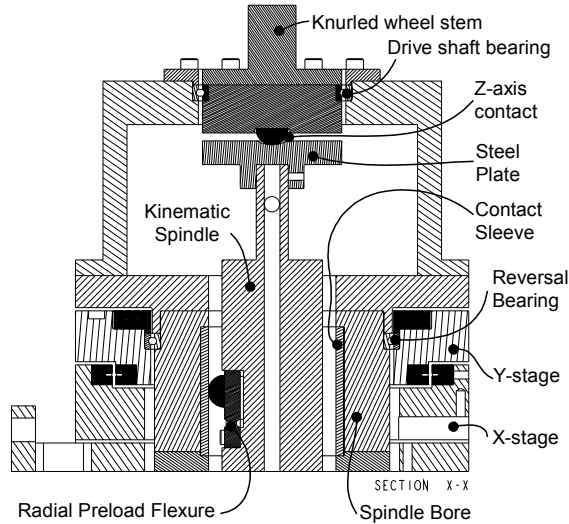


**Fig 2: Cross Section of Spindle and Drive System**

Two linear translation stages, X-stage and Y-stage, provide a method to align the instrument's axis of rotation with the axis of the test bore. The stages travel a maximum of 6.35 mm on crossed roller bearings. Micrometers allow precise positioning of both stages. A gothic-arch rolling element bearing accommodates reversal by enabling a 180-degree angular rotation of the spindle's support structure (contact sleeve, spindle bore, and Z-axis contact).

### Reversal and Error Separation

Conventional, fixed sensitive direction, roundness testers require reversing sensor orientation [7]. A rotating sensitive direction roundness tester, however, relies upon reversing the orientation of the tester (but not the sensor) in relation to the bore.

Reversal retains applicability for rotating sensitive direction roundness testing if it can be shown that reversing one set-up orientation eliminates one set of errors via addition or subtraction of gauge expressions. Fig 3 illustrates the reversal method for the prototype instrument. It is necessary that the probe's starting position be the same for both initial and reversal orientations.

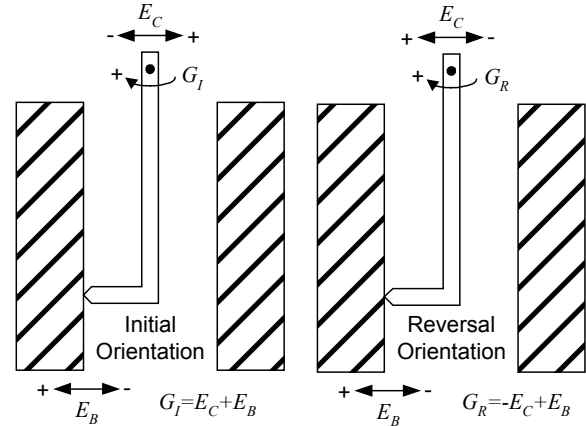


**Fig 3: Reversal for Rotating Sensitive Direction**

The reversal procedure inverts the spindle's error motion,  $E_C$ , while the orientation of the test bore and its roundness errors,  $E_B$ , remain constant. The gauge reading before reversal,  $G_I$ , and after reversal,  $G_R$ , are given in Eqs (1) and (2).

$$G_I = E_C + E_B \quad (1)$$

$$G_R = -E_C + E_B \quad (2)$$

Adding and subtracting the gauge readings gives the separated error expressions for  $E_B$  and  $E_C$  shown in Eqs (3) and (4).

$$E_B = \frac{1}{2}(G_I + G_R) \quad (3)$$

$$E_C = \frac{1}{2}(G_I - G_R) \quad (4)$$

### Kinematic Spindle Arrangement

The kinematic spindle relies upon exact constraint to position and orient its axis of rotation in space. Only five contacts are used, thereby allowing one degree of freedom in the spindle: rotation about its axis. As illustrated in Fig 4,  $P_{C1}$  is defined as the Z-axis constraint and is located on the spindle's axis of rotation. Four other contact points ( $P_{C2}$ ,  $P_{C3}$ ,  $P_{C4}$ ,  $P_{C5}$ ) are placed in high and low contact planes (HCP

and LCP). In each contact plane, two spheres are separated by 90 degrees, on the shaft's cylindrical surface. .

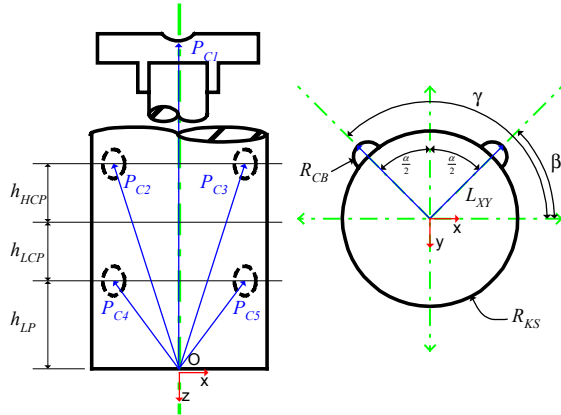


**Fig 4: Contact Locations on Kinematic Spindle**

The shaft rotates within a sleeve, creating a point-contact bearing. Tungsten carbide will likely be used for both the sleeve and contact hemispheres  $P_{C2}$  through  $P_{C5}$  due to its beneficial wear properties, low coefficient of friction, and high stiffness. The axial contact  $P_{C1}$  is a steel hemisphere contacting a steel plate for two reasons: 1) a larger coefficient of friction for steel on steel and 2) the ferromagnetic properties for the Z-axis preload. A radial compressive preload is established on contacts  $P_{C2}$  through  $P_{C5}$  using a flexure equipped with a contact hemisphere as seen in Fig 1. The contact between the preload flexure's hemisphere and the contact sleeve is termed  $P_{C6}$ , and it is centered between the contact planes and is aligned with the Y-axis.

### Spindle Drive Arrangement

Torque transmitted through the shaft's Z-axis constraint rotates the kinematic spindle. This arrangement, illustrated in Fig 5, is preferable to belt-drive since it does not impart radial forces, which are a source of error motion [5].

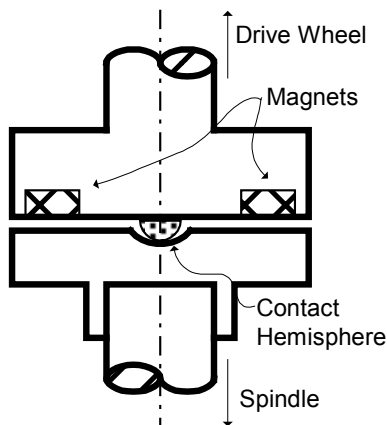


**Fig 5: Z-axis Contact and Drive Arrangement**

The maximum transmissible torque is derived from the surface traction between the axial contact hemisphere and the steel plate. The peak traction depends upon the radius of the contact area, the coefficient of friction, and the magnetic preload between the plates. The drive arrangement is successful when the transmitted torque is greater than the opposing moment generated by friction at the radial contact hemispheres  $P_{C2}$  through  $P_{C5}$  and  $P_{C6}$  against the contact sleeve.

### Magnetic Force Experiment

The magnetic force for a given separation between plates was empirically tested using the setup shown in Fig 6. An array of 3 and an array of 6 evenly spaced neodymium magnets ( $\phi 12.7$  mm x 6.35 mm) were fixed in an aluminum plate matching the configuration in the instrument. A 1018 carbon steel plate was attached to a Sensotec model 31 load-cell. The plate and load cell assembly were bolted to vertical translation stages.

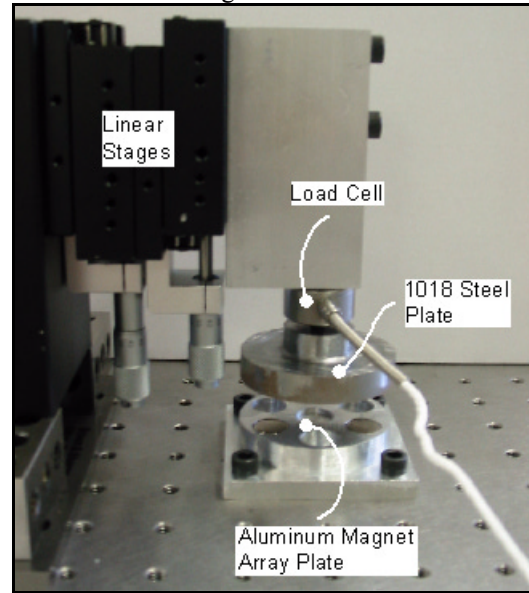


**Fig 6: Magnetic Force Experiment Setup**

Using a 1.27 mm (0.050") gauge block to establish parallelism, the steel plate was lowered to a known distance away from the magnetic plate. The load cell subsequently measured the force acting on the steel plate by the magnets at 0.5 mm increments up to 32mm. The experiment was executed thrice for each magnet array.

The mean of the three measurements are plotted in Fig 7 for the 3 and 6 magnet arrangements. Three magnets produced roughly 44 N and six magnets doubled the force to 88 N at the minimum offset of 1.27 mm. Dividing the six-magnet force curve by

two and plotting the result against the three-magnet force curve validated this relation.

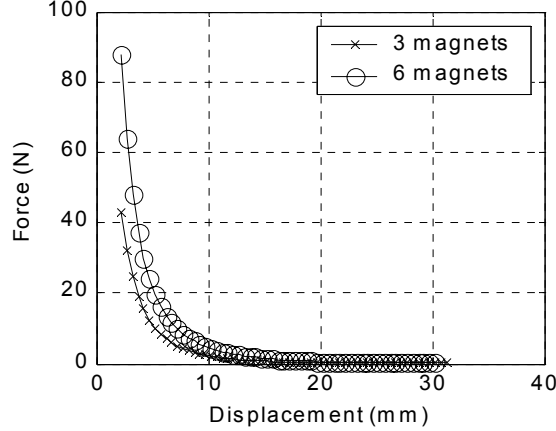


**Fig 7: Magnet Force as Function of Displacement**

### Analysis of Surface Traction

Hertzian contact analysis [8] provides a value for the contact radius,  $a$ , as a function of normal force,  $P$ , chosen from data gathered in the mag2netic force experiment. The analysis is based on the method described by Johnson [8]. Eq (5) gives the rotation angle,  $\beta$ , as a function the contact radius,  $a$ , shear moduli of the contacting materials,  $G_1$  and  $G_2$ , and the applied moment  $M_z$ .

$$\beta = \frac{3}{16} \left( \frac{1}{G_1} + \frac{1}{G_2} \right) \frac{M_z}{a^3} \quad (5)$$

Once  $\beta$  is known, the radius of the slip annulus region,  $c$ , may be calculated using Eq (6a).  $K(k)$  and  $E(k)$  are elliptical integrals of the first and second kind, respectively, evaluated for  $k$  given in Eq (6b). MATLAB or another computational method is helpful in solving for  $c$ .

$$\frac{3}{4\pi} \left( 1 - \frac{c^2}{a^2} \right) \left( \frac{1}{G_1} + \frac{1}{G_2} \right) [K(k) - E(k)] = \frac{a^2 \beta}{\mu P} \quad (6a)$$

$$k = \left( 1 - c^2 / a^2 \right)^{1/2} \quad (6b)$$

Two functions exist for the traction between contacting bodies: 1) the region of no-slip from the center of the contact area to the slip annulus, and 2) the region between the slip annulus and the perimeter of the contact area. Within the slip annulus, the traction,  $q(r)$ , is given by Eq (7), and beyond the annulus, the traction is given by Eq (8).

$$q(r) = \frac{3M_z r}{4\pi a^3} (a^2 - r^2)^{-1/2} \quad \text{for } 0 \leq r < c \quad (7)$$

$$q(r) = \frac{3\mu P}{2\pi a^3} (a^2 - r^2)^{1/2} \quad \text{for } c \leq r \leq a \quad (8)$$

The plot in Fig 8 illustrates the form of these functions for a particular preload. The traction increases until the slip annulus,  $c$ , is reached. It then jumps to a peak value and quickly decays to zero at the contact boundary,  $a$ . Increasing the magnetic preload,  $P$ , increases  $a$ , and the jump at  $c$  diminishes slightly.

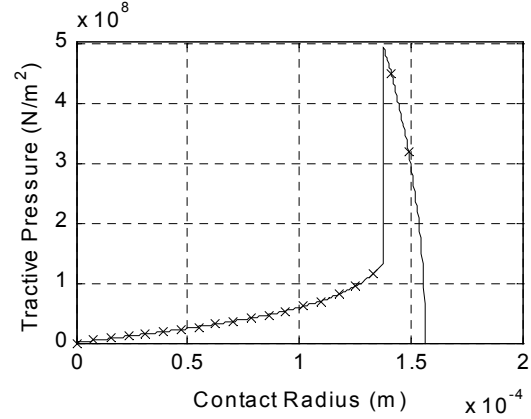


**Fig 8: Surface Traction**

### Magnetic Preload versus Critical Flexure Preload

The spindle's radial preload, supplied by a flexure, should be sized such that frictional forces acting at the contacts  $P_{C2}$  through  $P_{C6}$  do not create a moment greater than the drive arrangement can overcome. The flexure preload at which the drive arrangement begins to freely slide is defined as the critical flexure preload.

Johnson's expression for the maximum moment,  $M_z$ , transmissible through the drive arrangement is given in Eq (9) [8]. This expression shows that the torque is directly proportional to the coefficient of friction,  $\mu$ , and the preload force,  $P$ .

$$M_z = 3\pi\mu Pa / 16 \quad (9)$$

Eq (9) is used with an expression for spindle contact frictional forces to create a function of the radial preload imparted by the flexure. Using a MATLAB optimization routine, the critical flexure preload may be calculated as a function of the magnetic Z-axis preload.

Fig 9 plots the critical flexure preload versus the magnetic preload on the Z-axis contact. The coefficient of friction between  $P_{C1}$  through  $P_{C5}$  and  $P_{C6}$  and the spindle sleeve is varied to demonstrate the advantages of choosing a low-friction material for this application.

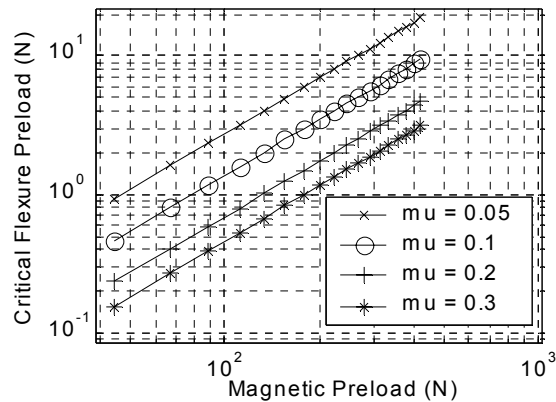


**Fig 9: Critical Flexure Preload as Function of Magnetic Axial Preload Force**

### Conclusions and Future Work

Since Hii demonstrated that kinematic spindles could achieve low asynchronous error but higher synchronous error, they may be applied with a reversal technique to construct a portable roundness instrument. Because it is necessary to maintain low asynchronous error for successful reversal, it is crucial to drive the spindle in a manner that introduces little or no disturbance forces to the shaft. This can be achieved with a point-contact drive system.

From this work, a number of generalizations are made regarding the design of such a drive system. A critical design aspect is the amount of torque transmissible through  $P_{CI}$  and its steel-plate companion. Increasing the magnetic preload on the steel plate and increasing the coefficient of friction at the radial contact points increase this transmitted torque. Increasing the magnetic preload causes the area beneath the surface traction curve to increase, and hence the moment that may be passed through the contact point.

The magnetic preload could be increased through several methods:

1. Increase the number of magnets in the array to achieve the desired preload,
2. Increase the size of the magnets used,
3. Custom manufacture a neodymium ring to match the diameter of the 1018 steel plate.

The  $P_{CI}$  contact hemisphere will likely be steel rather than tungsten carbide. The coefficient of friction for steel on steel contact is fairly high (~0.80).

For near point contact drive of a kinematic spindle, the friction at the radial contact points,  $P_{CI}$  through  $P_{C5}$  and  $P_{C6}$ , must be minimized to allow maximum radial preload. Maximized radial preload is desirable for a robust construction and a stable

spindle. Materials with low coefficients of friction, such as tungsten carbide ( $\mu=0.25$ ), may be a suitable choice for the contact hemispheres and contact sleeve.

Since spindle repeatability is necessary for reversal techniques to function properly, a wear study of the tungsten carbide contact hemispheres and sleeve will be undertaken. Wearing in either of these surfaces changes the spindle's asynchronous error pattern. In addition, characterization of the proposed contact probe (Mitutoyo SurfTest SJ-400) is required.

### Acknowledgements

The authors acknowledge encouragement from Bob Wasilesky at Mitutoyo for considering the application of kinematic spindles in roundness metrology.

### References

- [1] "Measurement of Out-of-Roundness". ASME B89.3.1-1972. American Society of Mechanical Engineers. 1972.
- [2] Donaldson, R.R. "A Simple Method for Separating Spindle Error From Test Ball Roundness" *CIRP Annals*. V. 21. 1972.
- [3] Evans, Chris J. and J. Robert Hocken. "Self-Calibration: Reversal, Redundancy, Error Separation, and Absolute Testing." *CIRP Annals*, V.45, N.2. 1996.
- [4] Blanding, D.L. *Exact Constraint: Machine Design Using Kinematics Principles*. ASME Press. New York. 1999.
- [5] Hii, King-Fu. *Kinematically Constrained Spindles*. M.S. Thesis. University of Kentucky. 2002.
- [6] K-F. Hii, E. Wolsing, R. Vallance, "Design of a Kinematic Spindle for Low-Force, Low-Speed Applications," *Proceedings of 16<sup>th</sup> Annual Meeting of the American Society for Precision Engineering*. ASPE. Crystal City, VA. November 10<sup>th</sup> – 15<sup>th</sup>, 2001.
- [7] "Axes of Rotation – Methods for Specifying and Testing". ASME 89.3.4-1985. American Society of Mechanical Engineers. 1985.
- [8] Johnson, K.L. *Contact Mechanics*. Cambridge University Press. Cambridge. 1985.